



## Article

# Rosemary (*Rosmarinus officinalis* L.) Glycolic Extract Protects Liver Mitochondria from Oxidative Damage and Prevents Acetaminophen-Induced Hepatotoxicity

Natalia S. S. Guimarães <sup>1</sup>, Vytória S. Ramos <sup>1</sup>, Laura F. L. Prado-Souza <sup>2</sup>, Rayssa M. Lopes <sup>2</sup> , Gabriel S. Arini <sup>3</sup>, Luís G. P. Feitosa <sup>3</sup>, Ricardo R. Silva <sup>3</sup>, Iseli L. Nantes <sup>2</sup>, Debora C. Damasceno <sup>4</sup>, Norberto P. Lopes <sup>3</sup> and Tiago Rodrigues <sup>1,\*</sup>

<sup>1</sup> Interdisciplinary Center of Biochemistry Investigation, University of Mogi das Cruzes (UMC), Mogi das Cruzes CEP 08780-911, SP, Brazil

<sup>2</sup> Center for Natural and Human Sciences, Federal University of ABC, Santo André CEP 09210-580, SP, Brazil

<sup>3</sup> NPPNS, Department of Biomolecular Sciences, Faculty of Pharmaceutical Sciences of Ribeirão Preto, University of São Paulo, Ribeirão Preto CEP 14040-900, SP, Brazil

<sup>4</sup> Laboratory of Experimental Research on Gynecology and Obstetrics, Sao Paulo State University (UNESP), Botucatu CEP 18618-687, SP, Brazil

\* Correspondence: tiago.rodrigues@ufabc.edu.br; Tel.: +55-(11)-4996-8371

**Abstract:** *Rosmarinus officinalis* L. (rosemary) is an aromatic culinary herb. Native to the Mediterranean region, it is currently cultivated worldwide. In addition to its use as a condiment in food preparation and in teas, rosemary has been widely employed in folk medicine and cosmetics. Several beneficial effects have been described for rosemary, including antimicrobial and antioxidant activities. Here, we investigated the mechanisms accounting for the antioxidant activity of the glycolic extract of *R. officinalis* (*Ro*) in isolated rat liver mitochondria (RLM) under oxidative stress conditions. We also investigated its protective effect against acetaminophen-induced hepatotoxicity in vivo. A crude extract was obtained by fractionated percolation, using propylene glycol as a solvent due to its polarity and cosmeceutical compatibility. The quantification of substances with recognized antioxidant action revealed the presence of phenols and flavonoids. Dereplication studies carried out through LC-MS/MS and GC-MS, supported by The Global Natural Product Social Molecular Networking (GNPS) platform, annotated several phenolic compounds, confirming the previous observation. In accordance, *Ro* decreased the production of reactive oxygen species (ROS) elicited by Fe<sup>2+</sup> or *t*-BOOH and inhibited the lipid peroxidation of mitochondrial membranes in a concentration-dependent manner in RLM. Such an effect was also observed in liposomes as membrane models. *Ro* also prevented the oxidation of mitochondrial protein thiol groups and reduced glutathione (GSH). In model systems, *Ro* exhibited a potent scavenger activity toward 2,2'-diphenyl-1-picrylhydrazyl (DPPH) radicals and superoxide anions. It also demonstrated an Fe<sup>2+</sup> chelating activity. Moreover, *Ro* did not exhibit cytotoxicity or dissipate the mitochondrial membrane potential ( $\Delta\Psi$ ) in rat liver fibroblasts (BRL3A cells). To evaluate whether such antioxidant protective activity observed in vitro could also be achieved in vivo, a well-established model of hepatotoxicity induced by acute exposure to acetaminophen (AAP) was used. This model depletes GSH and promotes oxidative-stress-mediated tissue damage. The treatment of rats with 0.05% *Ro*, administered intraperitoneally for four days, resulted in inhibition of AAP-induced lipid peroxidation of the liver and the prevention of hepatotoxicity, maintaining alanine and aspartate aminotransferase (ALT/AST) levels equal to those of the normal, non-treated rats. Together, these findings highlight the potent antioxidant activity of rosemary, which is able to protect mitochondria from oxidative damage in vitro, and effects such as the antioxidant and hepatoprotective effects observed in vivo.

**Keywords:** antioxidant; acetaminophen; hepatoprotection; mitochondria; oxidative stress; rosemary



**Citation:** Guimarães, N.S.S.; Ramos, V.S.; Prado-Souza, L.F.L.; Lopes, R.M.; Arini, G.S.; Feitosa, L.G.P.; Silva, R.R.; Nantes, I.L.; Damasceno, D.C.; Lopes, N.P.; et al. Rosemary (*Rosmarinus officinalis* L.) Glycolic Extract Protects Liver Mitochondria from Oxidative Damage and Prevents Acetaminophen-Induced Hepatotoxicity. *Antioxidants* **2023**, *12*, 628. <https://doi.org/10.3390/antiox12030628>

Academic Editors: Alexandra Barbouti and Vlasios Goulas

Received: 28 January 2023

Revised: 26 February 2023

Accepted: 28 February 2023

Published: 3 March 2023



**Copyright:** © 2023 by the authors. Licensee MDPI, Basel, Switzerland. This article is an open access article distributed under the terms and conditions of the Creative Commons Attribution (CC BY) license (<https://creativecommons.org/licenses/by/4.0/>).

## 1. Introduction

The Lamiaceae family contains a set of plants, often cultivated as herbs, whose leaves can be used as seasonings and whose essential oils are used as flavors in cosmeceuticals [1]. Among these plants, *Rosmarinus officinalis* L. stands out. Popularly known as rosemary (or alecrim in Brazil), *R. officinalis* is native to the Mediterranean region and is currently found worldwide. It has been extensively studied for its use in food and as a spice and/or preservative, in which it operates by inhibiting microbial growth and oxidative reactions [2]. The study of medicinal plants and herbs has proved to be an efficient strategy for prospecting novel compounds with therapeutic potential [3,4]. In this regard, a large number of secondary metabolites have been isolated and identified from *Rosmarinus* spp., including essential oils, flavonoids, tannins, terpenes, and phenolic acids [5–7]. In addition, carnosol, carnosic acid, and rosmarinic acids, which are reported to be the main components of rosemary, account for many of its biological activities [8–10]. The production of these bioactive secondary metabolites by rosemary depends on several factors, such as the plant part, climatic conditions and soil nutrients, humidity, temperature, water availability, and others [11]. Due to the large number of chemical studies carried out on *R. officinalis*, we opted for a dereplication strategy to avoid re-isolations [12]. Hyphenated liquid chromatography with electrospray ionization mass spectrometry (LC-ESI-MS/MS) is currently the most suitable technique for metabolomics approaches [13]. However, when analyzing extracts with an antioxidative potential, it is important to follow the oxidation processes at the source of the ESI in detail since substances with a low oxidation potential can lose electrons, changing the expected mass balance and leading to erroneous interpretations of chemical structures [14,15].

Furthermore, *R. officinalis* has long been used as a medicinal plant. In this context, a plethora of biological effects and health benefits have been attributed to rosemary essential oil, leaf extracts, and isolated substances, including antibacterial [16–18], anti-fungal [19,20], anti-inflammatory [21,22], antiatherogenic [23,24], antiangiogenic [25,26], antihypertensive [27], antiulcer [28], anti-diabetic [29,30], anticancer [31], and other effects (reviewed elsewhere [32,33]). In addition to these effects, this plant is also well known for its powerful antioxidant activity (reviewed in [34]). This is expected, as phytochemical analyses of rosemary extracts and essential oils have revealed several substances with recognized antioxidant properties, such as flavonoids and phenolic compounds [35,36]. In fact, such antioxidant activities of *R. officinalis* might help to explain some of the biological effects described above. The pathophysiology of several human diseases is related to the overproduction of reactive oxygen species (ROS) or a decreased capacity of the antioxidant defense system, resulting in oxidative stress, cellular/tissue damage, and, ultimately, organ dysfunction [37]. In this regard, it has been shown that *R. officinalis* exhibits hepatoprotective effects in different models of xenobiotic-induced liver toxicity, including carbon tetrachloride (CCl<sub>4</sub>) [38–41], creosote [38], azathioprine [39], hexavalent chromium [40], streptozotocin [41], and cyclophosphamide [42]. However, its protective effect against acetaminophen-induced hepatotoxicity has not been clearly demonstrated yet. Acetaminophen (AAP) is an anti-inflammatory and anti-pyretic drug, and AAP overdose is associated with acute liver failure [43]. During cytochrome P<sub>450</sub> liver metabolism, AAP is transformed in the highly reactive metabolite N-acetyl-p-benzoquinone imine (NAPQI), which oxidizes GSH [44] and causes oxidative stress.

Although the antioxidant activity of *R. officinalis* has been extensively studied in several biological systems and toxicity models, its potential protective effect on mitochondria under oxidative stress conditions has not been investigated. Despite the central role they play in cellular metabolism and energy production, mitochondria are also often associated with oxidative status since superoxide radical anions (O<sub>2</sub><sup>•−</sup>) are continuously generated during electron transport in the respiratory chain. This radical is counteracted by the antioxidant defense system, with the reducing power provided by reduced glutathione (GSH) and NAD(P)H [45]. However, excessive O<sub>2</sub><sup>•−</sup> formation and, consequently, its conversion to hydrogen peroxide (H<sub>2</sub>O<sub>2</sub>), can produce the extremely reactive hydroxyl

radical ( $\bullet\text{OH}$ ) by means of the Fenton reactions, which are catalyzed by  $\text{Fe}^{2+}$  and other transition metals [46]. Thus, the investigation of the effects of *R. officinalis* in such a complex mitochondrial scenario can further elucidate the molecular mechanisms of antioxidant protection in biological systems. Here, we investigated the antioxidant properties of *R. officinalis* leaf extracts in rat liver mitochondria and addressed its protective effect against AAP-induced hepatotoxicity in rats.

## 2. Materials and Methods

### 2.1. Chemicals, Plant Source, and Extract Preparation

All reagents used in this study were of the highest commercially available grade of purity. Aqueous solutions were prepared using type I water obtained using a Milli-Q system (Millipore, USA). *Rosmarinus officinalis* L. species were collected in Brazil (GPS localization: 760 m, 23°29'40" S) during the winter (August) of 2018. After botanical identification, voucher specimens were deposited at the Herbarium Mogiense (University of Mogi das Cruzes, Brazil). After drying at 40 °C in a ventilated drying oven, 100 g of selected leaves were submitted to fractionated percolation using a mixture of propylene glycol/water (7/3) as solvent, resulting in 100 mL of *Rosmarinus officinalis* glycolic extract (*Ro*). This extract was considered a 100% crude extract for subsequent concentration calculations.

### 2.2. Isolation of Mitochondria, Animal Treatments, and Sample Preparation

Liver mitochondria were isolated from rats by differential centrifugation in isosmotic media, as previously described [47]. Adult male Wistar rats weighing approximately 180 g were randomly divided into four groups ( $n = 7$ ), kept in a 12/12 h light/dark cycle, and fed ad libitum. All experiments involving animals were conducted in accordance with the guide for the care and use of laboratory animals (NIH Guidelines) and were previously approved by the Animal Ethics Committee of University of Mogi das Cruzes (CEUA). In order to induce hepatotoxicity, the AAP group received a single dose of 900 mg/kg of acetaminophen (Sigma-Aldrich, St. Louis, MI, USA) intraperitoneally. Animals were sacrificed 4 h after drug administration. The control group (C) received the same volume of solvent used for AAP dissolution, i.e., dimethyl sulfoxide (DMSO; Sigma-Aldrich, USA). The other two groups received 0.1 mL of 0.5% *Ro* intraperitoneally once per day in the morning for four consecutive days. One of these groups (*Ro*/AAP) also received AAP on the last day, as described above, 4 h before sacrifice. The animals were anesthetized with xylazine (5 mg/kg) and ketamine (60 mg/kg) for cardiac blood collection. The blood was immediately centrifuged at  $700\times g$  for 5 min to achieve serum separation. For homogenate preparation, the livers were removed and cut into small fragments in a buffer containing 250 mmol/L sucrose, 1 mmol/L EGTA, and HEPES-KOH 10 mmol/L at a pH of 7.4 at 4 °C. After washing the samples twice with the same medium, the tissues were homogenized using a Potter-Elvehjem. This was followed by centrifugation at  $580\times g$  for 5 min at 4 °C. The supernatant, called a homogenate, was immediately frozen at  $-70\text{ }^{\circ}\text{C}$  for subsequent experiments.

### 2.3. Preparation of PCPECL Liposomes

The phospholipids phosphatidylcholine, phosphatidylethanolamine, and cardiolipin (PCPECL, 5:3:2 ratio) were dissolved in  $\text{CHCl}_3$ , which was further evaporated under argon flux. The lipidic film was hydrated with 10 mM of cold sodium phosphate buffer at a pH of 7.4 and vortexed. To obtain the liposome solution (1 mM), lipids were submitted to sonication for 30 min at 4 °C using a Ney Ultrasonik (J. M. Ney Co., Bloomfield, CT, USA).

### 2.4. Total Phenols and Flavonoids

The soluble phenol derivatives were estimated using the Folin-Ciocalteu method [48] and expressed as  $\mu\text{M}$  of gallic acid equivalents based on a standard curve [49]. For flavonoid quantification, an aliquot was incubated in a medium containing 60  $\mu\text{L}$  of glacial acetic acid, 1.0 mL of pyridine  $\text{H}_2\text{O}:\text{AlCl}_3$  12% solution (17:80:3), and 1.24 mL of  $\text{DMSO}:\text{H}_2\text{O}$

(1:1) for 5 min at 25 °C. The absorbance of the chromophore produced in this reaction was determined spectrophotometrically at 420 nm, and the flavonoid content was determined based on a standard curve and expressed as  $\mu\text{M}$  of quercetin equivalents.

#### 2.5. DPPH Assay, $\text{Fe}^{2+}$ , and Superoxide Scavenger Activity

The reduction of the 1,1'-diphenyl-2-picrylhydrazyl radical (DPPH, Sigma-Aldrich, USA) by *Ro* was accompanied by photometric measurement in a UV1800 spectrophotometer (Shimadzu, Kyoto, Japan). An amount of 1.5 mL of 40 mM sodium acetate pH 5.5 was mixed into the reaction with 1.0 mL of absolute ethanol containing DPPH to achieve a final concentration of 0.1 mM. After incubation with different *Ro* concentrations for 5 min at 25 °C, the final absorbance was measured at 517 nm. Quercetin (Q, Sigma-Aldrich, USA) was used as reference. The amount of  $\text{Fe}^{2+}$  was quantified photometrically at 535 nm using 0.2 mM bathophenanthroline disulfonic acid (Sigma-Aldrich, USA) [50] in a competitive assay with *Ro*. At last, the xanthine/xanthine oxidase system was used to generate  $\text{O}_2^{\bullet-}$ . The scavenger activity of *Ro* was estimated by the inhibition of the nitroblue tetrazolium (NBT, Sigma-Aldrich, USA) reduction. After adding 0.08 U/mL xanthine oxidase to a phosphate buffer at a pH of 7.5, which contained 0.05 mM EDTA, 0.2 mM hypoxanthine, and 0.1 mM NBT, the absorbance was measured at 540 nm after 20 min of incubation at 37 °C (Shimadzu UV1800 Spectrophotometer, Tokyo, Japan).

#### 2.6. Reactive Oxygen Species (ROS)

The production of mitochondrial ROS was estimated kinetically using 2',7'-dichlorodihydrofluorescein diacetate ( $\text{H}_2\text{DCFDA}$ , Sigma-Aldrich, USA) [51], as previously described [52]. Briefly, mitochondria (1 mg/mL) were incubated in a buffer containing 125 mM sucrose, 65 mM KCl, and 10 mM HEPES-KOH at a pH of 7.4, plus 1  $\mu\text{M}$   $\text{H}_2\text{DCFDA}$  at 30 °C, under continuous stirring in the presence of 5 mM potassium succinate (Sigma-Aldrich, USA) (plus 2  $\mu\text{M}$  rotenone, Sigma-Aldrich, USA). The fluorescence emissions were recorded in a Hitachi F-2500 Spectrophotometer (Tokyo, Japan) at 503/529 nm for excitation/emission wavelength pairs, respectively.

#### 2.7. Lipid Oxidation

The liposomes (1 mM), mitochondria (1 mg/mL), or liver homogenates (1 mg/mL) were incubated with or without different *Ro* concentrations at 37 °C for 30 min, and with 50  $\mu\text{M}$   $\text{Fe}(\text{NH}_4)_2(\text{SO}_4)_4$  (plus 2.0 mM sodium citrate) or 0.6 mM *t*-BOOH as inducers of oxidative stress. Following incubation, for a thiobarbituric acid reactive substances (TBARS) assay, 1% thiobarbituric acid (TBA, Sigma-Aldrich, USA) was prepared by adding 50 mM NaOH, 15  $\mu\text{L}$  of 10 M NaOH, and 75  $\mu\text{L}$  of 20%  $\text{H}_3\text{PO}_4$  to each sample, followed by further incubation for 20 min at 85 °C. The MDA-TBA complex was extracted with 2 mL of *n*-butanol, and the absorbance was measured at 535 nm. The TBARS were calculated from  $\epsilon = 1.56 \times 10^5 \text{ M}^{-1} \cdot \text{cm}^{-1}$ , as described in [53]. Lipid hydroperoxides (LOOH) were also quantified in isolated mitochondria using xylene orange, as previously described in [54]. When applied, the percentages of inhibition by *Ro* were calculated in relation to positive controls (*t*-BOOH or  $\text{Fe}^{2+}$ ) which were considered to achieve 100% inhibition.

#### 2.8. GSH and Protein Thiol Groups

After 30 min of incubation at 37 °C in a medium containing 125 mM sucrose, 65 mM KCl, and 10 mM HEPES-KOH at a pH of 7.4, plus 5.0 mM potassium succinate and 2.0  $\mu\text{M}$  rotenone, the mitochondrial suspensions or liver homogenates were treated with 0.5 mL of 13% trichloroacetic acid and centrifuged at  $400 \times g$  for 5 min. For the GSH assay, aliquots (100  $\mu\text{L}$ ) of the supernatant were mixed with 1.8 mL of a 0.1 M sodium phosphate buffer at a pH of 8.0 containing 5 mM EGTA plus 100  $\mu\text{L}$  of 1 mg/mL *o*-phthalaldehyde (Sigma-Aldrich, USA). After 15 min of incubation, the fluorescence emissions were detected at 350/420 nm (excitation/emission) in a Hitachi F-2500 (Japan) fluorescence spectrophotometer [55]. The reduced thiol groups of proteins were quantified using 5,5'-dithiobis(2-

nitrobenzoic acid) (DTNB, Sigma-Aldrich, USA) [56]. The pellet obtained from the acid precipitation described above was suspended with 1 mL of a 0.5 M potassium phosphate buffer at a pH of 7.6 which contained 0.7% SDS. After adding 100  $\mu$ M DTNB, the absorbance was measured at 412 nm and the amount of the reduced thiol groups was calculated from  $\epsilon = 13,600 \text{ M}^{-1} \cdot \text{cm}^{-1}$  [57].

## 2.9. Cell Culture and Cellular Assays

BRL 3A cells (CRL-1442, ATCC) were cultivated in high-glucose Dulbecco's modified Eagle's medium (DMEM; Sigma-Aldrich, USA) supplemented with 10% fetal bovine serum (FBS) (Gibco, Thermo Fischer Scientific, Waltham, MA, USA), 100 U/mL penicillin, and 100  $\mu$ g/mL streptomycin at 37 °C in a 5% CO<sub>2</sub> atmosphere (Panasonic MCO-19AIC incubator, Osaka, Japan). Cells were used for the experiments during 4–8 passages after thawing. For the experiments, cells were washed twice with a calcium- and magnesium-free buffered saline solution (CMF-BSS), detached from the flasks using trypsin/EDTA (Gibco, Thermo Fischer Scientific, USA), and suspended in the supplemented medium. For the viability assay, cells ( $5 \times 10^4$  cells/cm<sup>2</sup>) were added to 96-well microplates (0.2 mL final volume) and incubated with different concentrations of Ro for 24 h. After adding 0.25 mg/mL MTT [3-(4,5-dimethylthiazol-2-yl)-2,5-diphenyl-2H-tetrazolium bromide] (Sigma-Aldrich, USA), 4 h of incubation, and the solubilization of formazan crystals, the absorbance of each well was measured at 570 nm in a Biotek ELX 800 microplate reader (BioTek Instruments, Winooski, VT, USA). Cell viability was determined relative to the control (absence of Ro), which was considered to have a 100% viability [58]. The mitochondrial transmembrane potential in the BRL 3A cells was estimated using fluorescence microscopy. Cells ( $5 \times 10^4$  cells/cm<sup>2</sup>) were seeded in 3.5 cm glass dishes (with a 0.17 mm thick cover glass on the bottom (Greiner Bio-One, Frickenhausen, Germany) and loaded with 40 nM DiOC<sub>6</sub>(3) (Thermo Fisher Scientific, USA) and 5 nM Hoechst 33258 (Thermo Fisher Scientific, USA) with incubation at 37 °C for 30 min. Images were acquired in a widefield Leica AF6000 microscope (Leica Microsystems, Wetzlar, Germany), using the HCX APO UVI 100 $\times$ /1.3 oil plan apochromatic objective and the ultrafast Leica DFC365 FX monochromatic digital camera (Leica Microsystems, Germany). The set of cube filters used included A4 (ex 360/40, DC 400 nm, em 470/40) and L5 (ex 480/40, DC 505, em 527/30) (Leica Microsystems, Germany) filters.

## 2.10. Blood Biochemical Analyses

Aspartate aminotransferase (AST) and alanine aminotransferase (ALT) were determined in serum using commercial kits according to the manufacturer's instructions (LABTEST, Lagoa Santa, MG, Brazil).

## 2.11. Untargeted Metabolomics Analysis by HPLC-ESI-MS/MS

An HPLC-MS analysis was performed in a Shimadzu UFLC system coupled to a quadrupole time-of-flight mass spectrometer (micrOTOF QII, Bruker Daltonics, Billerica, MA, USA) using a C18 column (5  $\mu$ m, XB-C18 Kinetex, 100 $\text{\AA}$ , 150  $\times$  3 mm, Phenomenex). The mobile phase was composed of water (A) and MeOH (B), both with 0.1% formic acid, at a flow rate of 0.75 mL.min<sup>-1</sup>. The following gradient was employed: 0–23 min, 10–100% B; 23–26 min, 100% B; 26–27 min, 100–10% B; and 27–30 min, 10% B. The column oven was set to 45 °C, and an injection volume of 10  $\mu$ L was selected. Chromatograms were acquired in both positive and negative ionization modes, and the following parameters were employed for the mass spectrometer: end plate offset, 500 V; capillary voltage, 3200 V for negative mode and 3500 V for positive mode; nebulizer pressure, 4.5 bar; dry gas (N<sub>2</sub>) flow, 9 L.min<sup>-1</sup>; dry temperature, 200 °C; mass range,  $m/z$  150 to 1200; MS/MS scan mode; number of precursors, 3; exclusion activation, 1 spectrum; and exclusion release, 36 s.

## 2.12. Gas Chromatography-Mass Spectrometry (GC-MS) Analysis

The glycolic extract was submitted to a head space analysis, and the GC-MS methodology was based on the previously reported methodology [59]. The analysis was carried

out on the GCMS-QP2010 (Schimadzu, Japan) according to the following parameters: injector temperature, 250 °C; column temperature, 60 °C; heating ramp from 60 to 210 °C, at 3 °C/min, with a total time of 50 min; chromatographic column, DB-5, 30 m × 0.25 mm in diameter, 0.25 µm in thickness; and helium was used as the carrier gas under 79.7 kPa at 1.30 mL/min with a linear velocity of 41.6 cm/s, a 1 µL injection volume, and a 1:60 split.

### 2.13. Statistical Analyses

Quantitative data are presented as the mean ± SD of (at least) three independent experiments performed in triplicate. For multiple comparisons, a one-way ANOVA was used, followed by Tukey's post hoc test. The Prism 8.0 software (GraphPad Software Inc., La Jolla, CA, USA) was used to perform the data analyses. Statistical significance was defined as \* ( $p < 0.05$ ), \*\* ( $p < 0.01$ ), and \*\*\* ( $p < 0.001$ ).

## 3. Results

### 3.1. *Rosmarinus officinalis* Glycolic Extract (Ro) Protects Mitochondrial Lipids and Proteins from Oxidation

The production of mitochondrial ROS was evaluated through the kinetic measurement of dichlorofluorescein (DCF) fluorescence. When incubated with *t*-BOOH or  $\text{Fe}^{2+}$ , isolated rat liver mitochondria energized by succinate immediately increased the production of ROS. Due to the nature of the oxidative stress inducer, it was possible to observe that the fluorescence increase rate was faster for the  $\text{Fe}^{2+}$  (Figure 1B, black line) than for the *t*-BOOH (Figure 1A, red line). The preincubation of the mitochondrial suspension with *Ro* abolished the ROS production triggered by both inducers in a concentration-dependent manner. These effects were translated into the protection of mitochondrial membranes from oxidation by  $\text{Fe}^{2+}$  (squares, orange) or *t*-BOOH (circles, red), estimated by TBARS (Figure 1C). Moreover, the formation of  $\text{Fe}^{2+}$ -induced lipid hydroperoxides was inhibited by *Ro* at 0.025% (orange) and 0.05% (red) (Figure 1D). Such a lipid protective action exhibited by *Ro* was accompanied by the prevention of GSH oxidation by *t*-BOOH (Figure 1E) and the oxidation of reduced thiol groups of mitochondrial proteins by both *t*-BOOH (Figure 1F) and  $\text{Fe}^{2+}$  (Figure 1G) at the same concentrations.

Together, these results indicate the ability of *Ro* to protect mitochondria (and possibly cells) from oxidative damage, highlighting its potential to prevent pathological conditions and diseases associated with oxidative stress.

### 3.2. Iron (II) Chelating and Free Radical Scavenger Activity Account to the Antioxidant Protection Exhibited by *Ro*

The quantification of total phenols and flavonoids, substances with recognized antioxidant action, are presented in Table 1. In an attempt to provide further mechanistical insights regarding the antioxidant capacity of *Ro*, its ability to chelate  $\text{Fe}^{2+}$ , which is used here as inducer of oxidative stress, was investigated. In a competitive spectrophotometric assay using bathophenanthroline, *Ro* chelated more than 75% of the available  $\text{Fe}^{2+}$ , even at a lower concentration (Figure 2A). This may help to explain, at least partially, the protective effects observed in the Figure 1. Additionally, the free radical scavenger activity of *Ro* was investigated. As observed in Figure 2B, *Ro* reduced (scavenged) DPPH radicals in a concentration-dependent manner. At 0.025%, the effect was similar to 10 µM quercetin, a well-studied flavonoid known for its free radical scavenger activity and antioxidant properties [60]. Since DPPH is not a biological free radical, we also investigated the ability of *Ro* to scavenge  $\text{O}_2^{\bullet-}$  generated by the xanthine/xanthine oxidase system, using NBT as indicator [61]. *Ro* exhibited significant  $\text{O}_2^{\bullet-}$  scavenger activity at 0.05 and 0.01%, evaluated by the inhibition of NBT reduction by this radical. Finally, using a lipidic model system to mimic mitochondrial membranes [62], i.e., unsaturated PCPECL liposomes, it was possible to demonstrate that *Ro* prevents  $\text{Fe}^{2+}$ -induced lipid oxidation regardless of mitochondrial function or a dependence on mitochondrial constituents. Thus, the ability to scavenge free radicals and to block lipid peroxidation reactions contributed to *Ro*'s antioxidant activity and to the protective effects observed in mitochondria (Figure 1).

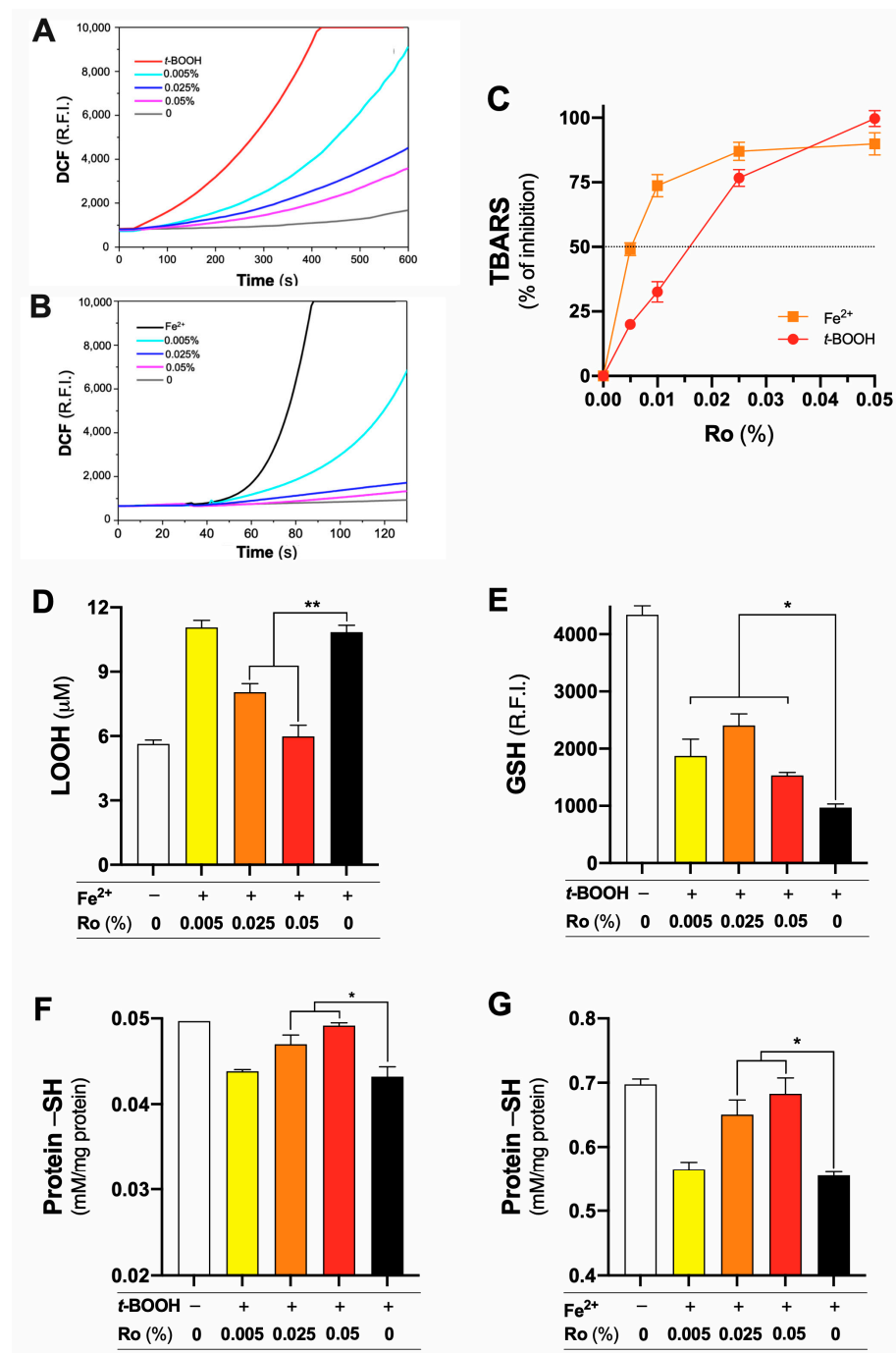


**Figure 1.** Glycolic extract of *Rosmarinus officinalis* (Ro) protects isolated rat liver mitochondria from oxidative stress. Mitochondria (1.0 mg/mL) were energized by succinate (site II substrate) in the presence of rotenone. DCF fluorescence was recorded kinetically using 0.6 mM *t*-BOOH ((A), red line) or 50 mM  $\text{Fe}^{2+}$  ((B), black line) as inducers of oxidative stress. Ro concentrations are represented by cyan (0.005%), blue (0.025%), and magenta (0.05%) lines. The inhibitory effect of Ro on the lipid oxidation (TBARS) induced by  $\text{Fe}^{2+}$  (squares, orange line) or *t*-BOOH (circles, red line). Effects of different concentrations of Ro on the formation of lipid hydroperoxides (LOOH) induced by  $\text{Fe}^{2+}$  (D), GSH oxidation induced by *t*-BOI (E), and oxidation of protein thiol groups induced by *t*-BOOH (F) or  $\text{Fe}^{2+}$  (G). In (D–G), negative control (absence of  $\text{Fe}^{2+}$  and Ro) is represented by white bars, positive control ( $\text{Fe}^{2+}$  or *t*-BOOH) by black bars, and the effects of Ro by yellow (0.005%), orange (0.025%), and red (0.05%) bars. In (C–G), data are presented as mean  $\pm$  SD of three independent experiments. Statistical differences are indicated by \* ( $p < 0.05$ ) and \*\* ( $p < 0.01$ ).

**Table 1.** Total phenols and flavonoids concentration present in 0.05% *Ro*.

	Concentration ( $\mu\text{M}$ )
Total phenols	$12.4 \pm 0.2$
Flavonoids	$7.2 \pm 0.1$

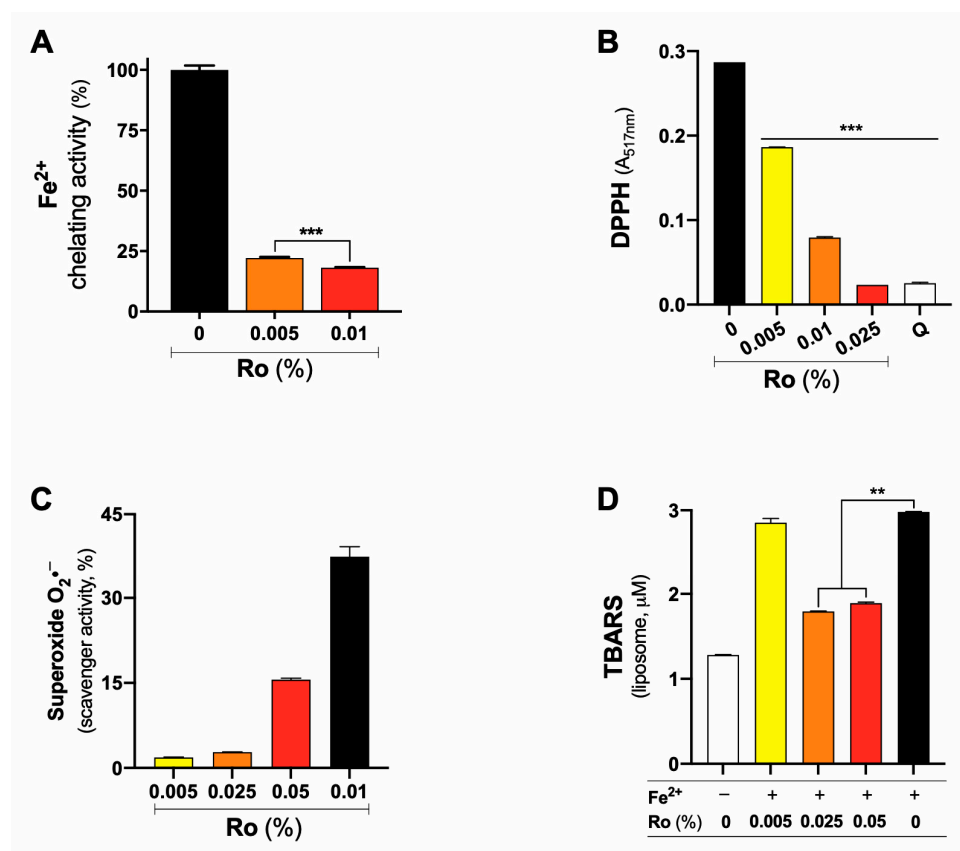


**Figure 2.** Fe<sup>2+</sup> chelating and free radical scavenger activities of glycolic extract of *Rosmarinus officinalis* (*Ro*). (A) 0.005 or 0.01% *Ro* were incubated with 50  $\mu\text{M}$   $\text{Fe}(\text{NH}_4)_2(\text{SO}_4)_2$  and the absorbance of bathophenanthroline-Fe<sup>2+</sup> complex was determined at 535 nm. (B) DPPH reduction by different *Ro* concentrations and the absorbance were determined at 517 nm, using 10  $\mu\text{M}$  quercetin (Q) as a reference. (C) Superoxide was detected by its reaction with nitroblue tetrazolium (NBT) at 540 nm, considered 100% in the absence of *Ro*; different indicated *Ro* concentrations decreased NBT reduction. (D) Inhibitory effect of *Ro* on the lipid oxidation (TBARS) of 1.0 mM PCPECL liposomes induced by Fe<sup>2+</sup>. Results expressed as percentage were calculated in relation to control (absence of *Ro* or Fe<sup>2+</sup>), considered to be 100%. Data are presented as mean  $\pm$  SD of three independent experiments. Statistical differences are indicated by \*\* ( $p < 0.01$ ) and \*\*\* ( $p < 0.001$ ).

### 3.3. *Ro* Does Not Affect Viability or Mitochondrial Membrane Potential ( $\Delta\Psi$ ) of Liver Fibroblasts

To strengthen the pharmacological potential of *Ro*, its cytotoxicity was evaluated *in vitro*. This is relevant since many antioxidant substances also have a cytotoxic effect [63] which can hinder their therapeutic potential. In this regard, the possible cytotoxicity of *Ro* was investigated in cultured BRL 3A cells, a fibroblast-like cell line isolated from rat livers. Cell viability, evaluated by the MTT assay, was not affected by *Ro* in the concentration range tested (0.005–0.05%), i.e., the incubation of *Ro* with BRL3A cells for 24 h did not decrease cell viability compared to the control (Figure 3A). These results were confirmed by the Trypan blue exclusion assay (Figure 3B). Moreover, *Ro* did not alter the  $\Delta\Psi$  of BRL 3A cells assessed by fluorescence microscopy using DiOC<sub>6</sub>(3) (Figure 3C(b),D, red bar). As a control, the total  $\Delta\Psi$  dissipation was achieved by adding CCCP, an uncoupler of the OXPHOS (Figure 3C(c),D, white bar).

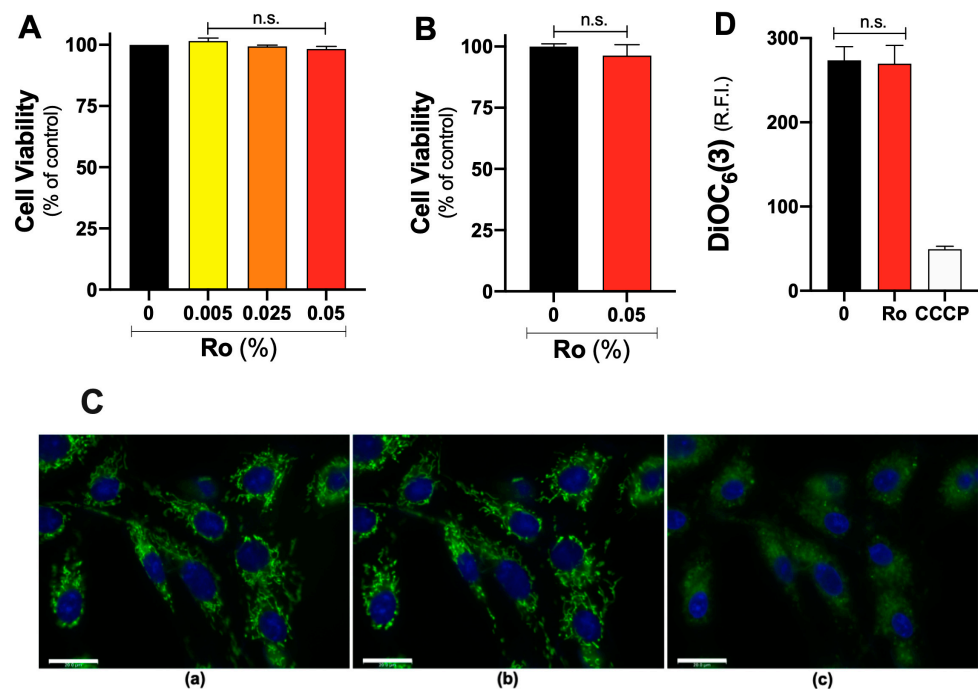


**Figure 3.** Absence of cytotoxicity of glycolic extract of *Rosmarinus officinalis* (Ro). **(A)** Viability of BRL 3A cells incubated with Ro (0 to 0.05%) for 24 h was estimated with MTT **(A)** and trypan blue **(B)** assays. The effects of Ro on cell viability were calculated in relation to control (absence of Ro), considered 100%. **(C)** Representative images of the mitochondrial membrane potential estimated by fluorescence microscopy using DiOC<sub>6</sub>(3). Cells were loaded with dyes, and fluorescence emission was acquired before and after 0.05% Ro addition. The uncoupler CCCP (10  $\mu$ M) was used as positive control (see Methods for details). Scale bars (20  $\mu$ m) **(D)** Relative quantification of DiOC<sub>6</sub>(3) fluorescence emission (L5 channel) considering the replicates. In **(A,B)** data are expressed as percentages of viable cells (mean  $\pm$  SD) calculated in relation to control (i.e., without Ro), considered as 100%. Statistically non-significant (n.s.), considering  $p < 0.05$ .

### 3.4. Ro Protection against Acetaminophen-Induced Hepatotoxicity in Rats

The antioxidant activity of Ro, its effect in protecting isolated rat liver mitochondria from oxidative stress conditions, and its absence of cytotoxicity in vitro led us to investigate whether such protective effects can be observed in vivo. To this end, a well-established and clinically relevant model of oxidative-stress-mediated hepatotoxicity was selected. The acute exposure to high doses of AAP generates radical intermediates during its hepatic metabolism, depleting antioxidant defenses and resulting in oxidative tissue damage [43]. To establish the experimental model, a single dose of AAP (900 mg/kg) was administered to the rats, which were or were not treated with 0.5% Ro, and the blood levels of alanine aminotransferase (ALT) and aspartate aminotransferase (AST) were analyzed. This high dose of AAP is well established in the literature to induce acute hepatotoxicity in mice and rats [64,65]. As expected, AAP administration increased serum levels of ALT (Figure 4A, black bar) and AST (Figure 4B, black bar), indicating the occurrence of liver injury. As a control, Ro alone did not exert any effect on ALT or AST levels (orange bars, Figure 4A,B, respectively) compared to the basal levels, i.e., control, non-treated rats (white bars, Figure 4A,B), indicating the absence of an intrinsic hepatotoxicity of the extract.

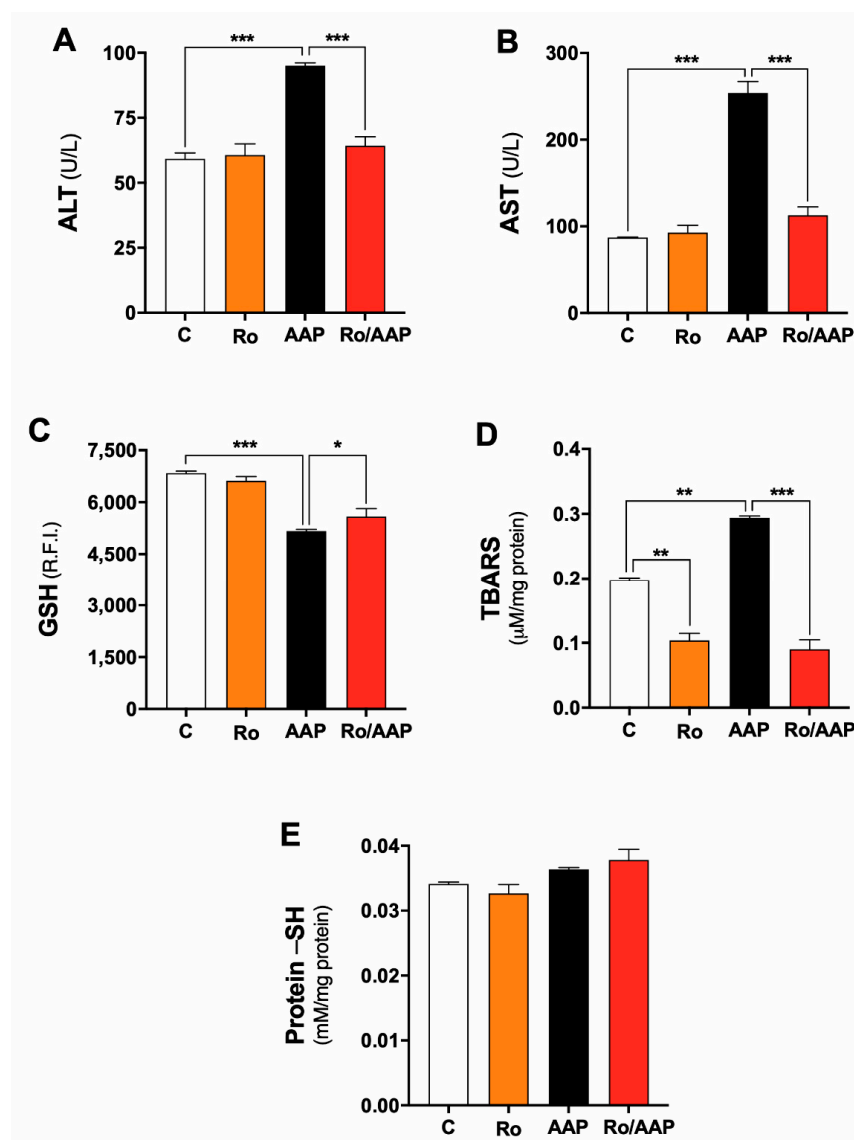
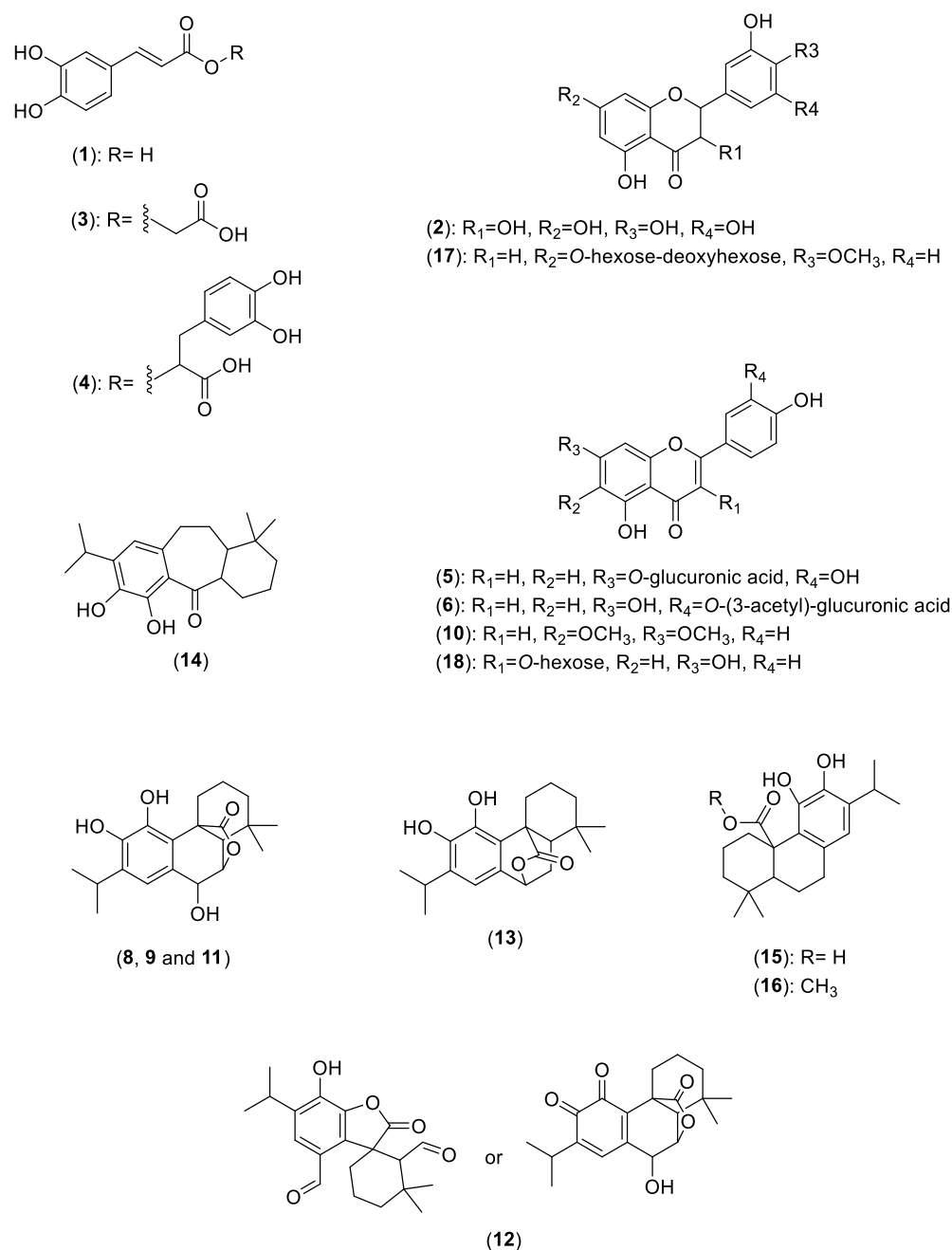


**Figure 4.** *Rosmarinus officinalis* (Ro) protects against acetaminophen-induced hepatotoxicity in vivo. Rats were divided into four groups (n = 7) and treated intraperitoneally, as described in Materials and Methods. Group C (white bars): control, treated with vehicle (DMSO); group Ro (orange bars): 0.5% Ro once a day for four days; group AAP (black bars): single dose of 900 mg/kg acetaminophen; group Ro/AAP (red bars): received Ro for four days, followed by single dose of AAP. (A) Alanine aminotransferase and (B) aspartate aminotransferase levels. (C) GSH, (D) TBARS, and (E) reduced thiol groups of proteins quantified as described by isolated mitochondria in Figure 1. Statistical differences are indicated by \* ( $p < 0.05$ ), \*\* ( $p < 0.01$ ), and \*\*\* ( $p < 0.001$ ).

Such a hepatotoxic effect of AAP was accompanied by GSH consumption (Figure 4C, black bar) and increased lipid oxidation (Figure 4D, black bar) without affecting the reduced thiol levels of proteins (Figure 4E, black bar). Interestingly, the treatment of animals with 0.5% Ro was able to reestablish the basal levels of ALT and AST in AAP-treated animals (red bars, Figure 4A,B, respectively), indicating a complete restoration of the liver integrity against the AAP-induced toxicity. We then further investigated whether this effect was accompanied by an improvement in oxidative stress indicators. In AAP-treated rats, Ro partially inhibited GSH oxidation (Figure 4C, red bar) and completely prevented lipid oxidation (Figure 4D, red bar) without an effect on the redox state of the protein thiol groups (Figure 4E, red bar). It is noteworthy that Ro diminished even the basal lipid oxidation (Figure 4D, orange bar).

### 3.5. Chemical Composition of *Rosmarinus officinalis* L. Glycolic Extract

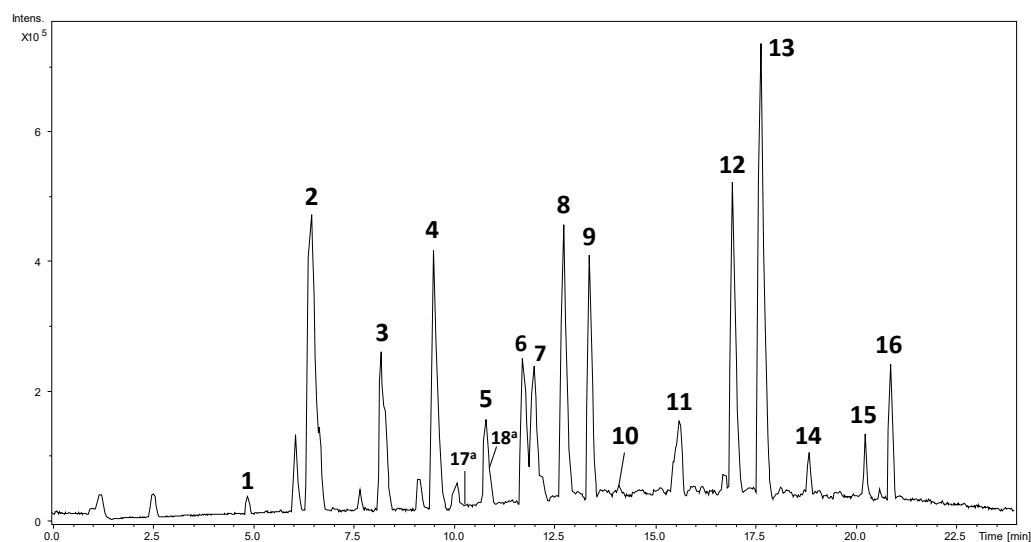
In order to gain more information about the chemical composition of *Ro*, we conducted an untargeted metabolomics analysis of the glycolic extract at both positive and negative ionization modes. The annotated metabolites are shown in Figure 5/ Table 2 and the ion intensity of each metabolite are presented in Figure 6. As expected, several phenolic compounds already described for this plant were detected [36], e.g., caffeic acid, rosmanol, and rosmarinic and carnosinic acids. All metabolites had their annotations confirmed through a detailed discussion of the decomposition reactions in the gaseous phase [66], following the correlation with the literature recently proposed by Pilon and collaborators [67] for the analysis of glycosylated flavonoids.



**Figure 5.** Chemical structures of compounds annotated in the *Ro* extract. Numbers in each structure refer to those presented in Table 2.

**Table 2.** Metabolites of Ro annotated by HPLC-ESI-MS/MS.

ID	RT (min)	MS $m/z$ [M – H] <sup>–</sup>	MS/MS $m/z$	Compound	Reference
1	4.9	179	135	Caffeic acid	[68]
2 <sup>a</sup>	6.5	305	225	Gallocatechin	[69]
3	8.2	237	179, 161	Caffeoylglycolic acid	-
4 <sup>a</sup>	9.4	359	161(100), 179, 197	Rosmarinic acid	[70]
5	10.8	461	285(100), 199, 151	Luteolin-7- <i>O</i> -glucuronide	[68]
6	11.7	503	399, 285(100), 255	Luteolin-3'- <i>O</i> -(3-acetyl)-glucuronide	[11]
7	12.0	315	300(100), 227, 199	Methoxy-tetrahydroxy-flavone	-
8 <sup>a</sup>	12.8	345	301, 283, 267, 217	Rosmanol isomer	[70]
9 <sup>a</sup>	13.4	345	283, 267, 227	Rosmanol isomer/epirosmanol	[70]
10	14.1	313	298, 283, 255, 227, 164	Cirsimaritin	[71] (CCM-SLIB00004718157)
11	15.6	345	283, 227	Rosmanol isomer/epirosmanol	[70]
12 <sup>a</sup>	16.9	343	299, 243, 216	Rosmadial or Rosmanol quinone	[68]
13 <sup>a</sup>	17.7	329	285(100), 201	Carnosol	[70]
14	18.9	315	285, 201	Rosmaridiphenol	[68]
15	20.3	331	287(100), 272, 244	Carnosic acid	[68]
16	20.9	345	301(100), 286, 271	Methyl carnosate	[70]
	RT (min)	MS $m/z$ [M + H] <sup>+</sup>	MS/MS $m/z$	Compound	Reference
17	10.3	611	547, 449, 287(100)	Hesperidin	[71] (CCM-SLIB00000214340)
18	10.8	449	287(100)	Astragalin	[71] (CCM-SLIB000003136634)

<sup>a</sup> Majority compounds—TIC (negative mode).**Figure 6.** Total Ion Chromatogram (TIC) of Ro obtained by LC-ESI-MS/MS analysis (negative mode).<sup>a</sup> Annotations from LC-ESI-MS/MS analysis in positive mode.

#### 4. Discussion

The wide range of biological actions reported for *R. officinalis* has long drawn the attention of researchers worldwide. In this study, for the first time, we showed that the antioxidant activity exhibited by rosemary extract and its chemical constituents is able to protect mitochondria subject to oxidative stress conditions. During the electron transport by the respiratory chain, mitochondria generate superoxide anions that are converted to hydrogen peroxide ( $\text{H}_2\text{O}_2$ ). In the presence of  $\text{Fe}^{2+}$ ,  $\text{H}_2\text{O}_2$  is converted to hydroxyl radicals, and these species are able to oxidize mitochondrial lipids and proteins, compromising energy production and  $\text{Ca}^{2+}$  homeostasis and culminating in cell death [46,72]. Thus, we used this complex system to evaluate the antioxidant potential of the glycolic extract of *R. officinalis* (Ro). Two different methods of inducing oxidative stress were used:  $\text{Fe}^{2+}$  and *t*-butyl hydroperoxide (*t*-BOOH). The former is able to catalyze Fenton reactions, amplifying the production of reactive oxygen species (ROS), and the latter is an organic peroxide that per se consumes antioxidant defenses to be eliminated, exposing cells to oxidative damage [45,46]. In both situations, Ro was able to inhibit ROS production and the oxidation of mitochondrial lipids and proteins. Previous studies have reported the ability of *R. officinalis* to inhibit the lipid peroxidation of phospholipids and membrane model systems [73–75], erythrocytes [76,77], low density lipoproteins (LDL) [78], and tissue homogenates [28].

Among the mechanisms of action for antioxidant activity, we found that Ro exhibits a free radical scavenger activity and the ability to chelate  $\text{Fe}^{2+}$ . Most studies have used a DPPH assay to infer the scavenger activity of rosemary extracts and essential oils; however, it is noteworthy that DPPH is not a radical produced in biological systems. Therefore, we further examined and demonstrated the capacity of the rosemary leaf glycolic extract to scavenge superoxide anions. Such an ability was previously shown for diterpenoids isolated from *R. officinalis* [79], and it is subject to seasonal variations [80]. The essential oil of *R. officinalis* was also able to scavenge hydroxyl radicals and chelate  $\text{Fe}^{2+}$  [81]. These properties of *R. officinalis* extracts are provided by their high content of powerful, well-known, synergistically acting antioxidant compounds including flavonoids, phenolic acids, and terpenes. For example, the antioxidant activity exhibited by carnosol was linked to an enhanced health and lifespan in *C. elegans*, accompanied by an increase in the activity of several antioxidant enzymes and a decrease in TBARS content [82]. As expected, the phytochemical analysis of the glycolic extract of *R. officinalis* identified the presence of several phenolic compounds already described for this plant. It should be noted that chlorogenic acid, a common compound with significant antioxidant activity, was not observed in these samples. A recent study demonstrated that the concentration of chlorogenic acid varies greatly depending on the drying process used for the leaves [83], which may explain, in part, the absence of the signal. The polyphenolic profile of rosemary has been widely described in the scientific literature [70,84–86], and the profile observed in the glycolic extract of the *R. officinalis* employed in this study was characterized by the presence of carnosic acid, carnosol, rosmarinic acid, and hesperidin. The mechanism of action was related to the free radicals' chain terminators and scavengers of ROS. On the other hand, compounds such as hesperidin are known for their ability to chelate metals. This confers a resistance to pests, as described in citrus [87], but can also support antioxidant properties. The occurrence of astragalin reinforces all the biological effects described in our article. This kaempferol 3-glucoside has several biological activities described, including antioxidant effects [88]. Therefore, the global analysis of the main metabolites contained in the extract support the observed activities. Finally, as expected, GC-MS exhibited a trace signal. The major compound detected was camphor, showing no contribution of the previous essential oil constituents to the described biological activities.

The antioxidant power of *R. officinalis* has been shown to be responsible for the plant's protective effects against oxidative stress. Rosemary prevented the renal toxicity elicited by diethylnitrosamine [89] and potassium dichromate [90] by inhibiting lipid peroxidation and improving the capacity of the antioxidant enzymatic system. Potassium dichromate

was also employed to induce hepatotoxicity in rats. In this context, rosemary essential oil exhibited hepatoprotective action, characterized by the inhibition of the lipid peroxidation, GSH, and protein oxidation, and by the restoration of the levels of antioxidant enzymes [40]. Similar observations were made for hepatotoxicity induced by  $\text{CCl}_4$ . Rosemary essential oil inhibited the lipid peroxidation and ‘reversed’ the activities of antioxidant enzymes catalase, peroxidase, glutathione peroxidase, and glutathione reductase in a liver homogenate [91]. A methanolic extract obtained from *R. officinalis* leaves [92,93] and a shoot tincture [94] also presented the same protective results on  $\text{CCl}_4$ -induced hepatotoxicity in rats. When *t*-BOOH was used as the oxidizing agent used to induce liver damage, *R. officinalis* also exhibited protective effects [95]. Acetaminophen is one of the most widely used analgesic and antipyretic drugs in the world. Although it is a relatively safe drug at therapeutic doses, acute overdose, chronic exposure, or association with other xenobiotics can result in severe hepatotoxicity. After oral intake, a major part of it is conjugated with glucuronic acid in the liver and eliminated by the kidneys. However, a fraction of AAP undergoes metabolism by the cytochrome  $\text{P}_{450}$  system, generating the toxic metabolite N-acetyl-p-benzoquinone imine (NAPQI) which, under normal conditions, is conjugated with GSH and eliminated. Nonetheless, increased NAPQI production results in the depletion of GSH and, consequently, oxidative liver damage [96]. Thus, we investigated for the first time the possible protective effect of *Ro* on AAP-induced hepatotoxicity. To validate the model, our data showed that a single high dose of AAP caused a depletion of GSH and increased lipid peroxidation. Such oxidative alterations were accompanied with liver damage. This was attested by increased levels of ALT and AST, biochemical markers of hepatocyte damage. Both aminotransferases were quantified since tissues other than the liver have elevated AST levels, such as the erythrocytes, heart, and muscle, while ALT has more specificity to the liver. Our data showed an increased AST/ALT ratio (De Ritis ratio), higher than 1.0, when rats were treated with AAP. This is predictive of long-term complications such as fibrosis and cirrhosis [97]. As shown, *Ro* indisputably protected the rat livers from AAP toxicity since the AST and ALT levels returned to the basal levels when compared to control. The powerful antioxidant activity of *Ro* seems to be responsible for this hepatoprotection since the GSH depletion was abolished and the lipid oxidation was also diminished. This strategy of using antioxidants to protect the liver from AAP toxicity was successfully achieved with N-acetyl cysteine [98,99].

Finally, it is important to correlate the general chemistry data annotated in this paper with the *Ro* effects. More than half of the compounds have the catechol group. It is well known that catechol and its many functionalized derivatives are excellent metal chelators [100]. Considering only the phenol group, which is a good and well-known antioxidant [100], the number is even more expressive since all 18 major compounds noted have at least one hydroxyl linked to an aromatic ring. Therefore, we believe that the observed effect must surely be a synergistic combination of all the actives described in this work.

## 5. Conclusions

Together, our data reinforced the antioxidant activity of *R. officinalis* through a free radical scavenger activity and by diminishing the  $\text{Fe}^{2+}$ -catalyzed Fenton reactions. We showed that these activities enabled *Ro* to protect isolated rat liver mitochondria from oxidative damage caused by different mechanisms ( $\text{Fe}^{2+}$  or *t*-BOOH). Moreover, *Ro* did not present cytotoxicity in cultured liver cells, and it exhibited a potent hepatoprotective effect against AAP toxicity in vivo. Further studies are necessary to the development of pharmaceutical formulations containing *Ro*, and clinical trials are required to evaluate the potential hepatoprotective effect in patients.

**Author Contributions:** Conceptualization, T.R.; formal analysis, T.R. and N.P.L.; investigation, N.S.S.G., V.S.R., L.F.L.P.-S., R.M.L., G.S.A., L.G.P.F. and R.R.S.; resources, I.L.N., D.C.D. and T.R.; data curation, N.S.S.G. and T.R.; writing—original draft preparation, N.P.L. and T.R.; writing—review and editing, I.L.N., D.C.D., N.P.L. and T.R.; visualization, N.S.S.G. and V.S.R.; supervision, T.R.; project administration, T.R.; funding acquisition, T.R. All authors have read and agreed to the published version of the manuscript.

**Funding:** This work was supported by the Fundação de Amparo à Pesquisa do Estado de São Paulo (FAPESP, 2008/01724-4; 2018/25747-5; 2020/02207-5; 2021/14650-3), the Coordenação de Aperfeiçoamento de Pessoal de Nível Superior (CAPES, Financial Code 001), and the Conselho Nacional de Desenvolvimento Científico e Tecnológico (CNPq, 312020/2019-8).

**Institutional Review Board Statement:** The study was conducted according to the guide for the care and use of laboratory animals (NIH guidelines), the Guiding Principles for Biomedical Research Involving Animals from the National Council for Animal Experimentation (CONCEA, Brazil) and approved by the Institutional Animal Care and Use Committee at the University of Mogi das Cruzes CEUA/UMC.

**Informed Consent Statement:** Not applicable.

**Data Availability Statement:** Not applicable.

**Acknowledgments:** We thank Carla T. Graves and Thiago E. R. dos Santos for the technical assistance with the animal manipulation and treatments. We also thank Marília Elias Gallon and Izabel Cristina Casanova Turatti for the technical assistance with the mass spectrometry experiments.

**Conflicts of Interest:** The authors declare no conflict of interest.

## References

- Ramos Da Silva, L.R.; Ferreira, O.O.; Cruz, J.N.; De Jesus Pereira Franco, C.; Oliveira Dos Anjos, T.; Cascaes, M.M.; Almeida Da Costa, W.; Helena De Aguiar Andrade, E.; Santana De Oliveira, M. *Lamiaceae* Essential Oils, Phytochemical Profile, Antioxidant, and Biological Activities. *Evid.-Based Complement. Altern. Med.* **2021**, *2021*, 6748052. [\[CrossRef\]](#)
- Veenstra, J.P.; Johnson, J.J. Rosemary (*Salvia rosmarinus*): Health-Promoting Benefits and Food Preservative Properties. *Int. J. Nutr.* **2021**, *6*, 1. [\[CrossRef\]](#) [\[PubMed\]](#)
- Gurib-Fakim, A. Medicinal Plants: Traditions of Yesterday and Drugs of Tomorrow. *Mol. Asp. Med.* **2006**, *27*, 1–93. [\[CrossRef\]](#) [\[PubMed\]](#)
- Boldi, A.M. Libraries from Natural Product-like Scaffolds. *Curr. Opin. Chem. Biol.* **2004**, *8*, 281–286. [\[CrossRef\]](#)
- Bouyahya, A.; Et-Touys, A.; Bakri, Y.; Talbaui, A.; Fellah, H.; Abrini, J.; Dakka, N. Chemical Composition of *Mentha pulegium* and *Rosmarinus officinalis* Essential Oils and Their Antileishmanial, Antibacterial and Antioxidant Activities. *Microb. Pathog.* **2017**, *111*, 41–49. [\[CrossRef\]](#) [\[PubMed\]](#)
- Mahmoud, A.A.; Al-Shihry, S.S.; Son, B.W. Diterpenoid Quinones from Rosemary (*Rosmarinus officinalis* L.). *Phytochemistry* **2005**, *66*, 1685–1690. [\[CrossRef\]](#)
- Borges, R.S.; Ortiz, B.L.S.; Pereira, A.C.M.; Keita, H.; Carvalho, J.C.T. *Rosmarinus officinalis* Essential Oil: A Review of Its Phytochemistry, Anti-Inflammatory Activity, and Mechanisms of Action Involved. *J. Ethnopharmacol.* **2019**, *229*, 29–45. [\[CrossRef\]](#) [\[PubMed\]](#)
- Bai, N.; He, K.; Roller, M.; Lai, C.S.; Shao, X.; Pan, M.H.; Ho, C.T. Flavonoids and Phenolic Compounds from *Rosmarinus officinalis*. *J. Agric. Food Chem.* **2010**, *58*, 5363–5367. [\[CrossRef\]](#)
- Jordán, M.J.; Castillo, J.; Bañón, S.; Martínez-Conesa, C.; Sotomayor, J.A. Relevance of the Carnosic Acid/Carnosol Ratio for the Level of Rosemary Diterpene Transfer and for Improving Lamb Meat Antioxidant Status. *Food Chem.* **2014**, *151*, 212–218. [\[CrossRef\]](#)
- Ibrahim, N.; Abbas, H.; El-Sayed, N.S.; Gad, H.A. *Rosmarinus officinalis* L. Hexane Extract: Phytochemical Analysis, Nanoencapsulation, and in Silico, in Vitro, and in Vivo Anti-Photoaging Potential Evaluation. *Sci. Rep.* **2022**, *12*, 13102. [\[CrossRef\]](#)
- Borrás-Linares, I.; Stojanović, Z.; Quirantes-Piné, R.; Arráez-Román, D.; Švarc-Gajić, J.; Fernández-Gutiérrez, A.; Segura-Carretero, A. *Rosmarinus officinalis* Leaves as a Natural Source of Bioactive Compounds. *Int. J. Mol. Sci.* **2014**, *15*, 20585–20606. [\[CrossRef\]](#) [\[PubMed\]](#)
- De Oliveira, G.G.; Carnevale Neto, F.; Demarque, D.P.; de Sousa Pereira-Junior, J.A.; Sampaio Peixoto Filho, R.C.; de Melo, S.J.; da Silva Almeida, J.R.G.; Lopes, J.L.C.; Lopes, N.P. Dereplication of Flavonoid Glycoconjugates from *Adenocalymma imperatoris-maximilianii* by Untargeted Tandem Mass Spectrometry-Based Molecular Networking. *Planta Med.* **2017**, *83*, 636–646. [\[CrossRef\]](#) [\[PubMed\]](#)
- Demarque, D.P.; Dusi, R.G.; de Sousa, F.D.M.; Grossi, S.M.; Silvério, M.R.S.; Lopes, N.P.; Espindola, L.S. Mass spectrometry-based metabolomics approach in the isolation of bioactive natural products. *Sci. Rep.* **2020**, *10*, 1051. [\[CrossRef\]](#)

14. Guaratini, T.; Vessecchi, R.L.; Lavarda, F.C.; Campos, P.M.B.G.M.; Naal, Z.; Gates, P.J.; Lopes, N.P. New chemical evidence for the ability to generate radical molecular ions of polyenes from ESI and HR-MALDI mass spectrometry. *Analyst* **2004**, *129*, 1223–1226. [\[CrossRef\]](#)
15. Guaratini, T.; Vessecchi, R.; Pinto, E.; Collepico, P.; Lopes, N.P. Balance of xanthophylls molecular and protonated molecular ions in electrospray ionization. *J. Mass Spectrom.* **2005**, *40*, 963–968. [\[CrossRef\]](#)
16. Bozin, B.; Mimica-Dukic, N.; Samojlik, I.; Jovin, E. Antimicrobial and Antioxidant Properties of Rosemary and Sage (*Rosmarinus officinalis* L. and *Salvia officinalis* L., Lamiaceae) Essential Oils. *J. Agric. Food Chem.* **2007**, *55*, 7879–7885. [\[CrossRef\]](#)
17. Wang, W.; Li, N.; Luo, M.; Zu, Y.; Efferth, T. Antibacterial Activity and Anticancer Activity of *Rosmarinus officinalis* L. Essential Oil Compared to That of Its Main Components. *Molecules* **2012**, *17*, 2704–2713. [\[CrossRef\]](#)
18. Moreno, S.; Scheyer, T.; Romano, C.S.; Vojnov, A.A. Antioxidant and Antimicrobial Activities of Rosemary Extracts Linked to Their Polyphenol Composition. *Free. Radic. Res.* **2006**, *40*, 223–231. [\[CrossRef\]](#) [\[PubMed\]](#)
19. Waller, S.B.; Cleff, M.B.; Dalla Lana, D.F.; de Mattos, C.B.; Guterres, K.A.; Freitag, R.A.; Sallis, E.S.V.; Fuentefria, A.M.; de Mello, J.R.B.; de Faria, R.O.; et al. Can the Essential Oil of Rosemary (*Rosmarinus officinalis* Linn.) Protect Rats Infected with Itraconazole-Resistant *Sporothrix Brasiliensis* from Fungal Spread? *J. Med. Mycol.* **2021**, *31*, 101199. [\[CrossRef\]](#)
20. Karpiński, T.M. Essential Oils of Lamiaceae Family Plants as Antifungals. *Biomolecules* **2020**, *10*, 103. [\[CrossRef\]](#)
21. Lucarini, R.; Bernardes, W.A.; Ferreira, D.S.; Tozatti, M.G.; Furtado, R.; Bastos, J.K.; Pauletti, P.M.; Januário, A.H.; Silva, M.L.A.E.; Cunha, W.R. In Vivo Analgesic and Anti-Inflammatory Activities of *Rosmarinus officinalis* Aqueous Extracts, Rosmarinic Acid and Its Acetyl Ester Derivative. *Pharm. Biol.* **2013**, *51*, 1087–1090. [\[CrossRef\]](#) [\[PubMed\]](#)
22. Ghasemzadeh Rahbardo, M.; Amin, B.; Mehri, S.; Mirnajafi-Zadeh, S.J.; Hosseinzadeh, H. Anti-Inflammatory Effects of Ethanolic Extract of *Rosmarinus officinalis* L. and Rosmarinic Acid in a Rat Model of Neuropathic Pain. *Biomed. Pharmacother.* **2017**, *86*, 441–449. [\[CrossRef\]](#) [\[PubMed\]](#)
23. Hsieh, C.L.; Peng, C.H.; Chyau, C.C.; Lin, Y.C.; Wang, H.E.; Peng, R.Y. Low-Density Lipoprotein, Collagen, and Thrombin Models Reveal That *Rosmarinus officinalis* L. Exhibits Potent Antiglycative Effects. *J. Agric. Food Chem.* **2007**, *55*, 2884–2891. [\[CrossRef\]](#) [\[PubMed\]](#)
24. Rodrigues, A.P.S.; Souza, B.S.F.E.; Barros, A.S.A.; de Oliveira Carvalho, H.; Duarte, J.L.; Boettger, L.E.M.; Barbosa, R.; Ferreira, A.M.; Ferreira, I.M.; Fernandes, C.P.; et al. The Effects of *Rosmarinus officinalis* L. Essential Oil and Its Nanoemulsion on Dyslipidemic Wistar Rats. *J. Appl. Biomed.* **2020**, *18*, 126–135. [\[CrossRef\]](#) [\[PubMed\]](#)
25. López-Jiménez, A.; García-Caballero, M.; Medina, M.Á.; Quesada, A.R. Anti-Angiogenic Properties of Carnosol and Carnosic Acid, Two Major Dietary Compounds from Rosemary. *Eur. J. Nutr.* **2013**, *52*, 85–95. [\[CrossRef\]](#)
26. Kayashima, T.; Matsubara, K. Antiangiogenic Effect of Carnosic Acid and Carnosol, Neuroprotective Compounds in Rosemary Leaves. *Biosci. Biotechnol. Biochem.* **2012**, *76*, 115–119. [\[CrossRef\]](#)
27. Karthik, D.; Viswanathan, P.; Anuradha, C.V. Administration of Rosmarinic Acid Reduces Cardiopathology and Blood Pressure through Inhibition of P22phox NADPH Oxidase in Fructose-Fed Hypertensive Rats. *J. Cardiovasc. Pharmacol.* **2011**, *58*, 514–521. [\[CrossRef\]](#)
28. Amaral, G.P.; de Carvalho, N.R.; Barcelos, R.P.; Dobrachinski, F.; de Lima Portella, R.; da Silva, M.H.; Lugokenski, T.H.; Dias, G.R.M.; da Luz, S.C.A.; Boligon, A.A.; et al. Protective Action of Ethanolic Extract of *Rosmarinus officinalis* L. in Gastric Ulcer Prevention Induced by Ethanol in Rats. *Food Chem. Toxicol.* **2013**, *55*, 48–55. [\[CrossRef\]](#)
29. Samarghandi, S.; Borji, A.; Farkhondeh, T. Evaluation of Antidiabetic Activity of Carnosol (Phenolic Diterpene in Rosemary) in Streptozotocin-Induced Diabetic Rats. *Cardiovasc. Haematol. Disord.-Drug Targets* **2017**, *17*, 11–17. [\[CrossRef\]](#)
30. Bakirel, T.; Bakirel, U.; Keleş, O.Ü.; Ülgen, S.G.; Yardibi, H. In Vivo Assessment of Antidiabetic and Antioxidant Activities of Rosemary (*Rosmarinus officinalis*) in Alloxan-Diabetic Rabbits. *J. Ethnopharmacol.* **2008**, *116*, 64–73. [\[CrossRef\]](#)
31. Tai, J.; Cheung, S.; Wu, M.; Hasman, D. Antiproliferation Effect of Rosemary (*Rosmarinus officinalis*) on Human Ovarian Cancer Cells in Vitro. *Phytomedicine* **2012**, *19*, 436–443. [\[CrossRef\]](#) [\[PubMed\]](#)
32. De Oliveira, J.R.; Camargo, S.E.A.; De Oliveira, L.D. *Rosmarinus officinalis* L. (Rosemary) as Therapeutic and Prophylactic Agent. *J. Biomed. Sci.* **2019**, *26*, 5. [\[CrossRef\]](#) [\[PubMed\]](#)
33. Sharifi-Rad, J.; Ezzat, S.M.; El Bishbishy, M.H.; Mnayer, D.; Sharopov, F.; Kılıç, C.S.; Neagu, M.; Constantin, C.; Sharifi-Rad, M.; Atanassova, M.; et al. Rosmarinus Plants: Key Farm Concepts towards Food Applications. *Phytother. Res.* **2020**, *34*, 1474–1518. [\[CrossRef\]](#) [\[PubMed\]](#)
34. Nieto, G.; Ros, G.; Castillo, J. Antioxidant and Antimicrobial Properties of Rosemary (*Rosmarinus officinalis*, L.): A Review. *Medicines* **2018**, *5*, 98. [\[CrossRef\]](#)
35. Dorta, D.J.; Pigoso, A.A.; Mingatto, F.E.; Rodrigues, T.; Pestana, C.R.; Uyemura, S.A.; Santos, A.C.; Curti, C. Antioxidant Activity of Flavonoids in Isolated Mitochondria. *Phytother. Res.* **2008**, *22*, 1213–1218. [\[CrossRef\]](#) [\[PubMed\]](#)
36. Okamura, N.; Haraguchi, H.; Hashimoto, K.; Yagi, A. Flavonoids in *Rosmarinus officinalis* Leaves. *Phytochemistry* **1994**, *37*, 1463–1466. [\[CrossRef\]](#)
37. Forman, H.J.; Zhang, H. Targeting Oxidative Stress in Disease: Promise and Limitations of Antioxidant Therapy. *Nat. Rev. Drug Discov.* **2021**, *20*, 689–709. [\[CrossRef\]](#)
38. El-Demerdash, F.M.; Abbady, E.A.; Baghdadi, H.H. Oxidative Stress Modulation by *Rosmarinus officinalis* in Creosote-Induced Hepatotoxicity. *Environ. Toxicol.* **2016**, *31*, 85–92. [\[CrossRef\]](#)

39. Amin, A.; Hamza, A.A. Hepatoprotective Effects of Hibiscus, Rosmarinus and Salvia on Azathioprine-Induced Toxicity in Rats. *Life Sci.* **2005**, *77*, 266–278. [\[CrossRef\]](#)
40. El-Demerdash, F.M.; El-Sayed, R.A.; Abdel-Daim, M.M. Hepatoprotective Potential of *Rosmarinus officinalis* Essential Oil against Hexavalent Chromium-Induced Hematotoxicity, Biochemical, Histological, and Immunohistochemical Changes in Male Rats. *Environ. Sci. Pollut. Res.* **2021**, *28*, 17445–17456. [\[CrossRef\]](#)
41. Ramadan, K.S.; Khalil, O.A.; Danial, E.N.; Alnahdi, H.S.; Ayaz, N.O. Hypoglycemic and Hepatoprotective Activity of *Rosmarinus officinalis* Extract in Diabetic Rats. *J. Physiol. Biochem.* **2013**, *69*, 779–783. [\[CrossRef\]](#) [\[PubMed\]](#)
42. El-Naggar, S.A.; Abdel-Farid, I.B.; Germoush, M.O.; Elgebaly, H.A.; Alm-Eldeen, A.A. Efficacy of *Rosmarinus officinalis* Leaves Extract against Cyclophosphamide-Induced Hepatotoxicity. *Pharm. Biol.* **2016**, *54*, 2007–2016. [\[CrossRef\]](#)
43. Bunchorntavakul, C.; Reddy, K.R. Acetaminophen-Related Hepatotoxicity. *Clin. Liver Dis.* **2013**, *17*, 587–607. [\[CrossRef\]](#) [\[PubMed\]](#)
44. Mazaleuskaya, L.L.; Sangkuhl, K.; Thorn, C.F.; Fitzgerald, G.A.; Altman, R.B.; Klein, T.E. PharmGKB Summary: Pathways of Acetaminophen Metabolism at the Therapeutic versus Toxic Doses. *Pharm. Genom.* **2015**, *25*, 416. [\[CrossRef\]](#)
45. Figueira, T.R.; Barros, M.H.; Camargo, A.A.; Castilho, R.F.; Ferreira, J.C.B.; Kowaltowski, A.J.; Sluse, F.E.; Souza-Pinto, N.C.; Vercesi, A.E. Mitochondria as a Source of Reactive Oxygen and Nitrogen Species: From Molecular Mechanisms to Human Health. *Antioxid. Redox Signal.* **2013**, *18*, 2029–2074. [\[CrossRef\]](#)
46. Sies, H. Oxidative Stress: Oxidants and Antioxidants. *Exp. Physiol.* **1997**, *82*, 291–295. [\[CrossRef\]](#)
47. Cruz, T.S.; Faria, P.A.; Santana, D.P.; Ferreira, J.C.; Oliveira, V.; Nascimento, O.R.; Cerchiaro, G.; Curti, C.; Nantes, I.L.; Rodrigues, T. On the Mechanisms of Phenothiazine-Induced Mitochondrial Permeability Transition: Thiol Oxidation, Strict Ca<sup>2+</sup> Dependence, and Cyt c Release. *Biochem. Pharmacol.* **2010**, *80*, 1284–1295. [\[CrossRef\]](#) [\[PubMed\]](#)
48. Ainsworth, E.A.; Gillespie, K.M. Estimation of total phenolic content and other oxidation substrates in plant tissues using Folin-Ciocalteu reagent. *Nat. Protoc.* **2007**, *2*, 875–877. [\[CrossRef\]](#) [\[PubMed\]](#)
49. Guimarães, N.S.S.; Mello, J.C.; Paiva, J.S.; Bueno, P.C.P.; Berretta, A.A.; Torquato, R.J.; Nantes, I.L.; Rodrigues, T. *Baccharis dracunculifolia*, the Main Source of Green Propolis, Exhibits Potent Antioxidant Activity and Prevents Oxidative Mitochondrial Damage. *Food Chem. Toxicol.* **2012**, *50*, 1091–1097. [\[CrossRef\]](#)
50. Cowart, R.E.; Singleton, F.L.; Hind, J.S. A Comparison of Bathophenanthrolinedisulfonic Acid and Ferrozine as Chelators of Iron(II) in Reduction Reactions. *Anal. Biochem.* **1993**, *211*, 151–155. [\[CrossRef\]](#)
51. Lebel, C.P.; Ischiropoulos, H.; Bondy, S.C. Evaluation of the probe 2',7'-dichlorofluorescein as an indicator of reactive oxygen species formation and oxidative stress. *Chem. Res. Toxicol.* **1992**, *5*, 227–231. [\[CrossRef\]](#) [\[PubMed\]](#)
52. Mello, J.C.; Guimarães, N.S.S.; Gonzalez, M.V.D.; Paiva, J.S.; Prieto, T.; Nascimento, O.R.; Tiago Rodrigues, T. Hydroxyl scavenging activity accounts for differential antioxidant protection of *Plantago major* against oxidative toxicity in isolated rat liver mitochondria. *J. Pharm. Pharmacol.* **2012**, *64*, 1177–1187. [\[CrossRef\]](#) [\[PubMed\]](#)
53. Mello, J.C.; Gonzalez, M.V.D.; Moraes, V.W.R.; Prieto, T.; Nascimento, O.R.; Rodrigues, T. Protective Effect of *Plantago major* Extract against *t*-BOOH-Induced Mitochondrial Oxidative Damage and Cytotoxicity. *Molecules* **2015**, *20*, 17747–17759. [\[CrossRef\]](#) [\[PubMed\]](#)
54. Borges, M.B.D.; Dos Santos, C.G.; Yokomizo, C.H.; Sood, R.; Vitovic, P.; Kinnunen, P.K.J.; Rodrigues, T.; Nantes, I.L. Characterization of Hydrophobic Interaction and Antioxidant Properties of the Phenothiazine Nucleus in Mitochondrial and Model Membranes. *Free. Radic. Res.* **2010**, *44*, 1054–1063. [\[CrossRef\]](#) [\[PubMed\]](#)
55. Hissin, P.J.; Hilf, R. A Fluorometric Method for Determination of Oxidized and Reduced Glutathione in Tissues. *Anal. Biochem.* **1976**, *74*, 214–226. [\[CrossRef\]](#)
56. Cálgaro-Helena, A.F.; Devienne, K.F.; Rodrigues, T.; Dorta, D.J.; Raddi, M.S.G.; Vilegas, W.; Uyemura, S.A.; Santos, A.C.; Curti, C. Effects of Isocoumarins Isolated from *Paepalanthus Bromelioides* on Mitochondria: Uncoupling, and Induction/Inhibition of Mitochondrial Permeability Transition. *Chem. Biol. Interact.* **2006**, *161*, 155–164. [\[CrossRef\]](#)
57. Jocelyn, P.C. Spectrophotometric Assay of Thiols. *Methods Enzymol.* **1987**, *143*, 44–67. [\[CrossRef\]](#)
58. Mello, J.C.; Moraes, V.W.R.; Watashi, C.M.; Silva, D.C.; Cavalcanti, L.P.; Franco, M.K.K.D.; Yokaichiya, F.; Araujo, D.R.; Rodrigues, T. Enhancement of chlorpromazine antitumor activity by Pluronic F127/L81 nanostructured system against human multidrug resistant leukemia. *Pharmacol. Res.* **2016**, *111*, 102–112. [\[CrossRef\]](#)
59. Pilon, A.C.; Del Grande, M.; Silvério, M.R.S.; Silva, R.R.; Albernaz, L.C.; Vieira, P.C.; Lopes, J.L.C.; Espindola, L.S.; Lopes, N.P. Combination of GC-MS Molecular Networking and Larvicidal Effect against *Aedes aegypti* for the Discovery of Bioactive Substances in Commercial Essential Oils. *Molecules* **2022**, *27*, 1588. [\[CrossRef\]](#)
60. Liu, Y.; Guo, M. Studies on Transition Metal-Quercetin Complexes Using Electrospray Ionization Tandem Mass Spectrometry. *Molecules* **2015**, *20*, 8583–8594. [\[CrossRef\]](#)
61. Hyung, S.C.; Jun, W.K.; Cha, Y.N.; Kim, C. A Quantitative Nitroblue Tetrazolium Assay for Determining Intracellular Superoxide Anion Production in Phagocytic Cells. *J. Immunoass. Immunochem.* **2006**, *27*, 31–44. [\[CrossRef\]](#)
62. Pessoto, F.S.; Faria, P.A.; Cunha, R.L.O.R.; Comasseto, J.V.; Rodrigues, T.; Nantes, I.L. Organotellurane-Promoted Mitochondrial Permeability Transition Concomitant with Membrane Lipid Protection against Oxidation. *Chem. Res. Toxicol.* **2007**, *20*, 1453–1461. [\[CrossRef\]](#) [\[PubMed\]](#)
63. Simunkova, M.; Barbierikova, Z.; Jomova, K.; Hudecova, L.; Lauro, P.; Alwasel, S.H.; Alhazza, I.; Rhodes, C.J.; Valko, M. Antioxidant vs. Prooxidant Properties of the Flavonoid, Kaempferol, in the Presence of Cu(II) Ions: A ROS-Scavenging Activity, Fenton Reaction and DNA Damage Study. *Int. J. Mol. Sci.* **2021**, *22*, 1619. [\[CrossRef\]](#) [\[PubMed\]](#)

64. Jeffery, E.H.; Haschek, W.M. Protection by dimethylsulfoxide against acetaminophen-induced hepatic, but not respiratory toxicity in the mouse. *Toxicol. Appl. Pharmacol.* **1988**, *93*, 452–461. [\[CrossRef\]](#)
65. Göksel Sener, G.; Sehirli, O.; Cetinel, S.; Yeğen, B.G.; Gedik, N.; Ayanoglu-Dülger, G. Protective effects of MESNA (2-mercaptoethane sulphonate) against acetaminophen-induced hepatorenal oxidative damage in mice. *J. Appl. Toxicol.* **2005**, *25*, 20–29. [\[CrossRef\]](#)
66. Lopes, N.P.; Stark, C.B.W.; Gates, P.J.; Staunton, J. Fragmentation studies on monensin A by sequential electrospray mass spectrometry. *Analyst* **2002**, *127*, 503–506. [\[CrossRef\]](#)
67. Pilon, A.C.; Gu, H.; Raftery, D.; Bolzani, V.D.S.; Lopes, N.P.; Castro-Gamboa, I.; Carnevale Neto, F. Mass Spectral Similarity Networking and Gas-Phase Fragmentation Reactions in the Structural Analysis of Flavonoid Glycoconjugates. *Anal. Chem.* **2019**, *91*, 10413–10423. [\[CrossRef\]](#)
68. Mena, P.; Cirlini, M.; Tassotti, M.; Herrlinger, K.A.; Dall'Asta, C.; Del Rio, D. Phytochemical Profiling of Flavonoids, Phenolic Acids, Terpenoids, and Volatile Fraction of a Rosemary (*Rosmarinus officinalis* L.) Extract. *Molecules* **2016**, *21*, 1576. [\[CrossRef\]](#)
69. Sharma, Y.; Velamuri, R.; Fagan, J.; Schaefer, J. Full-Spectrum Analysis of Bioactive Compounds in Rosemary (*Rosmarinus officinalis* L.) as Influenced by Different Extraction Methods. *Molecules* **2020**, *25*, 4599. [\[CrossRef\]](#)
70. Kontogianni, V.G.; Tomic, G.; Nikolic, I.; Nerantzaki, A.; Sayyad, A.; Stosic-Grujicic, N.; Stojanovic, S.; Gerothanassis, I.P.; Tzakos, A.G. Phytochemical profile of *Rosmarinus officinalis* and *Salvia officinalis* extracts and correlation to their antioxidant and anti-proliferative activity. *Food Chem.* **2013**, *136*, 120–129. [\[CrossRef\]](#)
71. Wang, M.; Carver, J.J.; Phelan, V.V.; Sanchez, L.M.; Garg, N.; Peng, Y.; Nguyen, D.D.; Watrous, J.; Kapono, C.A.; Luzzatto-Knaan, T.; et al. Sharing and community curation of mass spectrometry data with Global Natural Products Social Molecular Networking. *Nat. Biotechnol.* **2016**, *34*, 828–837. [\[CrossRef\]](#) [\[PubMed\]](#)
72. Green, D.R.; Reed, J.C. Mitochondria and Apoptosis. *Science* **1998**, *281*, 118. [\[CrossRef\]](#) [\[PubMed\]](#)
73. Aruoma, O.I.; Halliwell, B.; Aeschbach, R.; Löliger, J. Antioxidant and Pro-Oxidant Properties of Active Rosemary Constituents: Carnosol and Carnosic Acid. *Xenobiotica* **1992**, *22*, 257–268. [\[CrossRef\]](#)
74. Pérez-Fons, L.; Garzón, M.T.; Micol, V. Relationship between the Antioxidant Capacity and Effect of Rosemary (*Rosmarinus officinalis* L.) Polyphenols on Membrane Phospholipid Order. *J. Agric. Food Chem.* **2010**, *58*, 161–171. [\[CrossRef\]](#)
75. Harlina, P.W.; Ma, M.; Shahzad, R.; Khalifa, I. Effect of Rosemary Extract on Lipid Oxidation, Fatty Acid Composition, Antioxidant Capacity, and Volatile Compounds of Salted Duck Eggs. *Food Sci. Anim. Resour.* **2022**, *42*, 689–711. [\[CrossRef\]](#)
76. Nazem, F.; Farhangi, N.; Neshat-Gharamaleki, M. Beneficial Effects of Endurance Exercise with *Rosmarinus officinalis* Labiateae Leaves Extract on Blood Antioxidant Enzyme Activities and Lipid Peroxidation in Streptozotocin-Induced Diabetic Rats. *Can. J. Diabetes* **2015**, *39*, 229–234. [\[CrossRef\]](#) [\[PubMed\]](#)
77. Karimi, G.; Hassanzadeh, M.; Mehri, S. Protective Effect of *Rosmarinus officinalis* L. Essential Oil against Free Radical-Induced Erythrocyte Lysis. *Iran. J. Pharm. Sci.* **2005**, *1*, 231–236.
78. Kaliora, A.C.; Andrikopoulos, N.K. Effect of Alkanna Albugam Root on LDL Oxidation. A Comparative Study with Species of the Lamiaceae Family. *Phytother. Res.* **2005**, *19*, 1077–1079. [\[CrossRef\]](#)
79. Haraguchi, H.; Saito, T.; Okamura, N.; Yagi, A. Inhibition of Lipid Peroxidation and Superoxide Generation by Diterpenoids from *Rosmarinus officinalis*. *Planta Med.* **1995**, *61*, 333–336. [\[CrossRef\]](#)
80. Sueishi, Y.; Sue, M.; Masamoto, H. Seasonal Variations of Oxygen Radical Scavenging Ability in Rosemary Leaf Extract. *Food Chem.* **2018**, *245*, 270–274. [\[CrossRef\]](#)
81. Horvathova, E.; Navarova, J.; Galova, E.; Sevcovicova, A.; Chodakova, L.; Snahnicanova, Z.; Melusova, M.; Kozics, K.; Slamenova, D. Assessment of Antioxidative, Chelating, and DNA-Protective Effects of Selected Essential Oil Components (Eugenol, Carvacrol, Thymol, Borneol, Eucalyptol) of Plants and Intact *Rosmarinus officinalis* Oil. *J. Agric. Food Chem.* **2014**, *62*, 6632–6639. [\[CrossRef\]](#)
82. Lin, C.; Zhang, X.; Su, Z.; Xiao, J.; Lv, M.; Cao, Y.; Chen, Y. Carnosol Improved Lifespan and Healthspan by Promoting Antioxidant Capacity in *Caenorhabditis elegans*. *Oxidative Med. Cell. Longev.* **2019**, *2019*, 59580431619. [\[CrossRef\]](#) [\[PubMed\]](#)
83. Moreira, E.A.; Pilon, A.C.; Andrade, L.E.; Lopes, N.P. New Perspectives on Chlorogenic Acid Accumulation in Harvested Leaf Tissue: Impact on Traditional Medicine Preparations. *ACS Omega* **2018**, *3*, 12. [\[CrossRef\]](#)
84. Zegura, B.; Dobnik, D.; Niderl, M.H.; Filipi, M. Antioxidant and antigenotoxic effects of rosemary (*Rosmarinus officinalis* L.) extracts in *Salmonella typhimurium* TA98 and HepG2 cells. *Environ. Toxicol. Pharmacol.* **2011**, *32*, 296–305. [\[CrossRef\]](#) [\[PubMed\]](#)
85. Visentin, A.; Rodríguez-Rojo, S.; Navarrete, A.; Maestri, D.; Cocero, M.J. Precipitation and encapsulation of rosemary antioxidants by supercritical antisolvent process. *J. Food Eng.* **2012**, *109*, 9–15. [\[CrossRef\]](#)
86. Sasaki, K.; El Omri, A.; Kondo, S.; Han, J.; Isoda, H. *Rosmarinus officinalis* polyphenols produce anti-depressant like effect through monoaminergic and cholinergic functions modulation. *Behav. Brain Res.* **2013**, *238*, 86–94. [\[CrossRef\]](#)
87. Soares, M.S.; da Silva, D.F.; Forim, M.R.; da Silva, M.F.; Fernandes, J.B.; Vieira, P.C.; Silva, D.B.; Lopes, N.P.; de Carvalho, S.A.; de Souza, A.A.; et al. Quantification and localization of hesperidin and rutin in *Citrus sinensis* grafted on *C. limonia* after *Xylella fastidiosa* infection by HPLC-UV and MALDI imaging mass spectrometry. *Phytochemistry* **2015**, *115*, 161–170. [\[CrossRef\]](#) [\[PubMed\]](#)
88. Kluska, M.; Juszczak, M.; Żuchowski, J.; Stochmal, A.; Woźniak, K. Effect of Kaempferol and Its Glycoside Derivatives on Antioxidant Status of HL-60 Cells Treated with Etoposide. *Molecules* **2022**, *27*, 333. [\[CrossRef\]](#) [\[PubMed\]](#)
89. Hassanen, N.H.M.; Fahmi, A.; Shams-Eldin, E.; Abdur-Rahman, M. Protective Effect of Rosemary (*Rosmarinus officinalis*) against Diethylnitrosamine-Induced Renal Injury in Rats. *Biomarkers* **2020**, *25*, 281–289. [\[CrossRef\]](#)

90. El-Demerdash, F.M.; El-Sayed, R.A.; Abdel-Daim, M.M. *Rosmarinus officinalis* Essential Oil Modulates Renal Toxicity and Oxidative Stress Induced by Potassium Dichromate in Rats. *J. Trace Elem. Med. Biol.* **2021**, *67*, 126791. [[CrossRef](#)]
91. Rašković, A.; Milanović, I.; Pavlović, N.; Čebović, T.; Vukmirović, S.; Mikov, M. Antioxidant Activity of Rosemary (*Rosmarinus officinalis* L.) Essential Oil and Its Hepatoprotective Potential. *BMC Complement. Med. Ther.* **2014**, *14*, 225. [[CrossRef](#)] [[PubMed](#)]
92. Sotelo-Félix, J.I.; Martinez-Fong, D.; Muriel, P.; Santillán, R.L.; Castillo, D.; Yahuaca, P. Evaluation of the Effectiveness of *Rosmarinus officinalis* (Lamiaceae) in the Alleviation of Carbon Tetrachloride-Induced Acute Hepatotoxicity in the Rat. *J. Ethnopharmacol.* **2002**, *81*, 145–154. [[CrossRef](#)] [[PubMed](#)]
93. Gutiérrez, R.; Alvarado, J.L.; Presno, M.; Pérez-Veyna, O.; Serrano, C.J.; Yahuaca, P. Oxidative Stress Modulation by *Rosmarinus officinalis* in CCl<sub>4</sub>-Induced Liver Cirrhosis. *Phytother. Res.* **2010**, *24*, 595–601. [[CrossRef](#)]
94. Ielciu, I.; Sevastre, B.; Olah, N.K.; Turdean, A.; Chișe, E.; Marica, R.; Oniga, I.; Uifălean, A.; Sevastre-Berghian, A.C.; Niculae, M.; et al. Evaluation of Hepatoprotective Activity and Oxidative Stress Reduction of *Rosmarinus officinalis* L. Shoots Tincture in Rats with Experimentally Induced Hepatotoxicity. *Molecules* **2021**, *26*, 1737. [[CrossRef](#)] [[PubMed](#)]
95. Joyeux, M.; Rolland, A.; Fleurentin, J.; Mortier, F.; Dorfman, P. Tert-Butyl Hydroperoxide-Induced Injury in Isolated Rat Hepatocytes: A Model for Studying Anti-Hepatotoxic Crude Drugs. *Planta Med.* **1990**, *56*, 171–174. [[CrossRef](#)]
96. Siemionow, K.; Teul, J.; Dragowski, P.; Pałka, J.; Miltky, W. New Potential Biomarkers of Acetaminophen-Induced Hepatotoxicity. *Adv. Med. Sci.* **2016**, *61*, 325–330. [[CrossRef](#)]
97. Botros, M.; Sikaris, K.A. The De Ritis Ratio: The Test of Time. *Clin. Biochem. Rev.* **2013**, *34*, 117.
98. Corcoran, G.B.; Wong, B.K. Role of Glutathione in Prevention of Acetaminophen-Induced Hepatotoxicity by N-Acetyl-L-Cysteine in Vivo: Studies with N-Acetyl-D-Cysteine in Mice. *J. Pharmacol. Exp. Ther.* **1986**, *238*, 54–61.
99. Hjelle, J.J.; Brzeznicka, E.A.; Klaassen, C.D. Comparison of the Effects of Sodium Sulfate and N-Acetylcysteine on the Hepatotoxicity of Acetaminophen in Mice. *J. Pharmacol. Exp. Ther.* **1986**, *236*, 526–534.
100. Perron, N.R.; Brumaghim, J.L. A Review of the Antioxidant Mechanisms of Polyphenol Compounds Related to Iron Binding. *Cell Biochem. Biophys.* **2009**, *53*, 75–100. [[CrossRef](#)]

**Disclaimer/Publisher's Note:** The statements, opinions and data contained in all publications are solely those of the individual author(s) and contributor(s) and not of MDPI and/or the editor(s). MDPI and/or the editor(s) disclaim responsibility for any injury to people or property resulting from any ideas, methods, instructions or products referred to in the content.